



## Rab1a and Rab5a preferentially bind to binary lipid compositions with higher stored curvature elastic energy

Marie L. Kirsten, Rudi A. Baron, Miguel C. Seabra & Oscar Ces


**To cite this article:** Marie L. Kirsten, Rudi A. Baron, Miguel C. Seabra & Oscar Ces (2013) Rab1a and Rab5a preferentially bind to binary lipid compositions with higher stored curvature elastic energy, *Molecular Membrane Biology*, 30:4, 303-314, DOI: [10.3109/09687688.2013.818725](https://doi.org/10.3109/09687688.2013.818725)



**To link to this article:** <https://doi.org/10.3109/09687688.2013.818725>



 View supplementary material 

 Published online: 02 Jul 2013.

 Submit your article to this journal 

 Article views: 917

 View related articles 

 Citing articles: 3 View citing articles 

## Rab1a and Rab5a preferentially bind to binary lipid compositions with higher stored curvature elastic energy

MARIE L. KIRSTEN<sup>1,2,\*</sup>, RUDI A. BARON<sup>1†</sup>, MIGUEL C. SEABRA<sup>1,3</sup> & OSCAR CES<sup>2</sup>

<sup>1</sup>Molecular Medicine Section, National Heart and Lung Institute, Imperial College London, <sup>2</sup>Department of Chemistry, Institute of Chemical Biology, Imperial College London, UK, and <sup>3</sup>CEDOC, Faculdade de Ciências Médicas, Universidade Nova de Lisboa, Portugal

(Received 22 May 2013; and in revised form 17 June 2013)

### Abstract

Rab proteins are a large family of GTP-binding proteins that regulate cellular membrane traffic and organelle identity. Rab proteins cycle between association with membranes and binding to RabGDI. Bound on membranes, each Rab has a very specific cellular location and it is this remarkable degree of specificity with which Rab GTPases recognize distinct subsets of intracellular membranes that forms the basis of their ability to act as key cellular regulators, determining the recruitment of downstream effectors to the correct membrane at the correct time. The molecular mechanisms controlling Rab localization remain poorly understood. Here, we present a fluorescence-based assay to investigate Rab GTPase membrane extraction and delivery by RabGDI. Using EGFP-Rab fusion proteins the amount of Rab:GDI complex obtained by GDI extraction of Rab proteins from HEK293 membranes could be determined, enabling control of complex concentration. Subsequent partitioning of the Rab GTPases into vesicles made up of artificial binary lipid mixtures showed for the first time, that the composition of the target membrane plays a key role in the localization of Rab proteins by sensing the stored curvature elastic energy in the membrane.

**Keywords:** Lateral stress, protein-membrane interactions, membrane traffic

### Introduction

Rab GTPases form the largest subfamily of small GTPases and exhibit an average size of around 25 kDa. To date, approximately 70 members have been identified in humans, sharing around 30% sequence identity. They are key regulators of a broad range of membrane trafficking processes, such as vesicle budding and fusion, organelle motility, secretory pathways (Hutagalung and Novick 2011) and they also contribute to organelle identity (Zerial and McBride 2001). In addition to a number of Rab-related genetic diseases such as Choroideremia (Seabra et al. 1993) and Griscelli Syndrome (Barral et al. 2002), Rab proteins are increasingly implicated in cancer (Akavia et al. 2010, Hendrix et al. 2010) and infectious and inflammatory diseases (Jancic et al. 2007, Mizuno et al. 2007,

Lipinski et al. 2009, Yokoyama et al. 2011), as well as immunodeficiency (Johnson et al. 2010).

Rab GTPase activity is regulated by a binary conformational switch controlled by the guanine nucleotide status and by reversible membrane association (Ullrich et al. 1993), which is facilitated by insertion of hydrophobic C-terminal geranylgeranyl groups into the membrane. This Rab cycle is illustrated in Figure 1. In the active, GTP-bound form, Rab proteins interact with a plethora of effectors, reflecting their functional versatility (Hutagalung and Novick 2011). In the inactive, GDP-bound form, Rab proteins can be recruited into the cytosol by RabGDI (Guanine nucleotide dissociation inhibitor, hereafter called GDI). Two GDI isoforms exist in humans,  $\alpha$  and  $\beta$ , sharing 85% sequence identity (Nishimura et al. 1994). No clear difference in function between the two GDI isoforms has been identified, suggesting at

Correspondence: Dr Oscar Ces, Imperial College London, Department of Chemistry and Institute of Chemical Biology, Exhibition Road, SW7 2AZ London, UK. Tel: +44 (0) 20 7594 3754. E-mail: o.ces@imperial.ac.uk

\*Marie L. Kirsten is presently at EMBL Heidelberg, 69117 Heidelberg, Germany.

†Rudi A. Baron is presently at Cerenis Therapeutics, 31682 Labège, France.

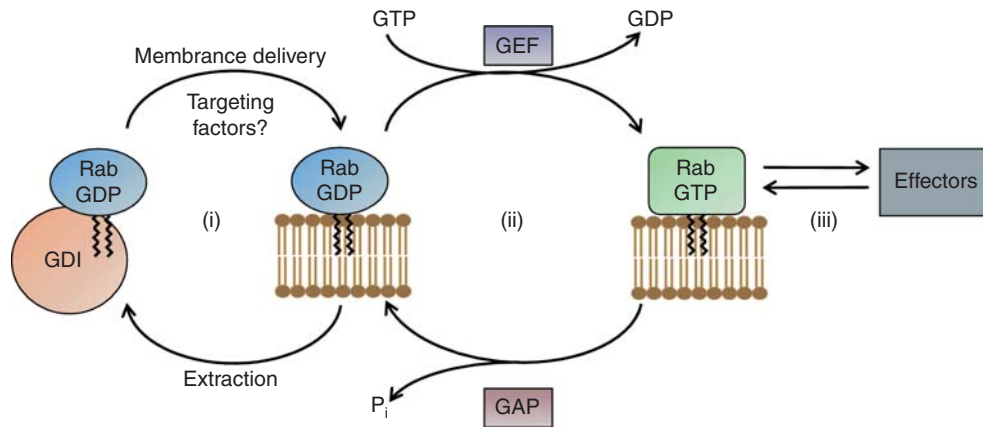


Figure 1. The Rab cycle. (i) GDI extracts inactive Rab proteins from membranes and cycles them between the cytosol and membrane association. (ii) Once membrane bound, the nucleotide is exchanged for GTP with the aid of Guanine nucleotide exchange factors (GEFs) rendering the Rab protein active. GTPase activating proteins (GAPs) increase the generally low intrinsic GTPase activity of Rab proteins to catalyse hydrolysis of GTP to return Rab proteins into their inactive state once their function on the membrane is fulfilled. (iii) In the active state Rab proteins interact with a number of diverse effectors. This Figure is reproduced in color in *Molecular Membrane Biology* online.

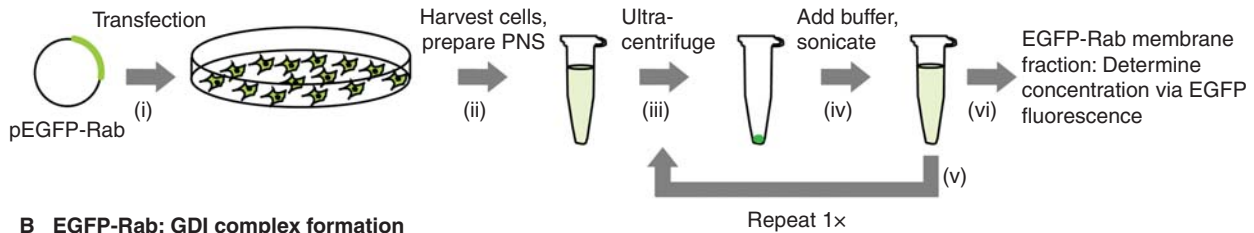
least some degree of redundancy. However, they exhibit tissue-specific expression levels, for example GDI $\alpha$  is predominantly expressed in brain tissue while GDI $\beta$  is ubiquitously expressed in all tissue types (Nishimura et al. 1994). GDI also delivers Rab proteins from the cytosol to the cytosolic face of subcellular membrane compartments, which they target with very high specificity (Lombardi et al. 1993, Soldati et al. 1994, Ullrich et al. 1994, Horiuchi et al. 1995, Wu et al. 2010).

Specific Rab family (RabF) and Rab subfamily (RabSF) regions have been shown to be crucial for correct targeting (Pereira-Leal and Seabra 2001, 2000), whereas the C-terminal hyper-variable regions do not convey the targeting signal (Ali et al. 2004). Multiple factors are thought to contribute to Rab recruitment to membranes (Pfeffer and Aivazian 2004, Seabra and Wasmeier 2004, Pfeffer 2005), including membrane-specific targeting factors and GDI displacement factors (GDFs) but identification of such factors has met with limited success. One of only two GDFs found to date is Yip3/PRA1 (yeast and human homologues, respectively), a membrane-bound protein which was shown to dissociate endosomal Rab5, Rab7 and Rab9 GDI complexes in solution, allowing nucleotide exchange (Dirac-Svejstrup et al. 1997, Sivars et al. 2003). The other protein exhibiting GDF activity toward the Rab1a: GDI complex, alongside Guanine nucleotide exchange factor (GEF) activity, is SidM (Machner and Isberg 2007). It has been suggested that interaction with downstream effectors of Rab proteins stabilizes them onto the correct membrane (Aivazian et al. 2006, Ganley and Pfeffer 2006), but overall the mechanisms that regulate the ability of Rab proteins to distinguish between different subcellular

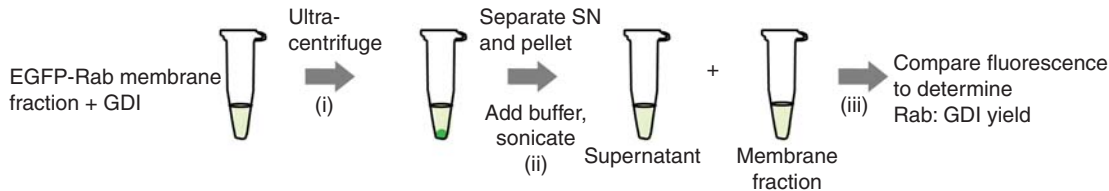
membranes with high specificity remain poorly understood. This includes the role played by membrane composition as a targeting factor. This is a damaging oversight as the broader literature contains a significant body of evidence that protein function in cells is often modulated by the physical properties of biological membranes. In particular, stored curvature elastic stress (Marsh 2006), surface charge density (Winterhalter and Helfrich 1988), and curvature (Lipowsky 1991) have been shown to regulate protein stability (Hong and Tamm 2004), folding (Booth 2000, Nagy et al. 2001, Seddon et al. 2008, Miller et al. 2009, Booth and Clarke 2010), binding (Lewis and Cafiso 1999, Bigay et al. 2005, Beck et al. 2008), and activity (Attard et al. 1998, 2000, Curnow et al. 2004, Charalambous et al. 2008) via well characterized coupling of proteins with lipid bilayers. Examples include proteins that are involved in lipid biosynthetic pathways and membrane trafficking such as CTP:phosphocholine cytidyltransferase (CCT) (Attard et al. 2000), the small Arf GTPases Arf1 (Beck et al. 2008) and Sar1p (Lee et al. 2005).

We present a novel approach for quantifying Rab GTPase membrane delivery, enabling the direct comparison of membrane partitioning of different Rab proteins to membranes of controlled composition. The assay allows investigation of Rab targeting in the presence and absence of additional targeting factors such as GDFs, GEFs, and effectors. GDFs have been proposed as a consequence of the high affinities of Rab proteins for GDI (Shapiro and Pfeffer 1995, Dirac-Svejstrup et al. 1997, Alexandrov et al. 1998, Wu et al. 2007). However, our findings suggest that in the presence of model membranes Rab:GDI dissociation and membrane association is sufficiently high and that the lipid composition of the target

### A Preparation of EGFP-Rab membrane fraction



### B EGFP-Rab: GDI complex formation



### C EGFP-Rab membrane delivery

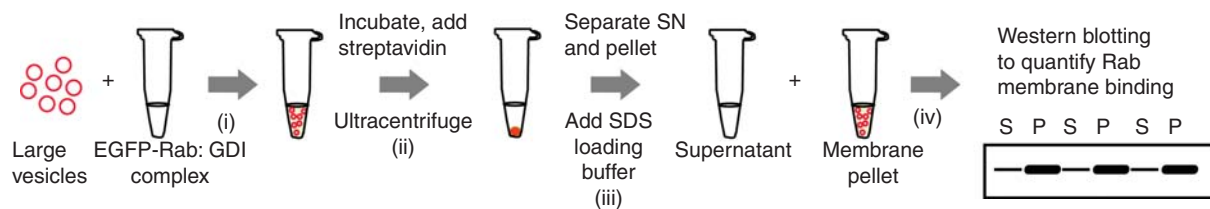


Figure 2. Schematic representation of experimental approach used to investigate Rab membrane targeting. (A) (i) EGFP-Rab fusion proteins were produced by overexpression in HEK293A cells. (ii) The cells were harvested, washed, lysed and the PNS was prepared by centrifugation. (iii) The membrane fraction was then obtained by ultracentrifugation of the PNS. (iv) The resulting membrane pellet was resuspended in buffer by sonication and (v) pelleted again by ultracentrifugation to reduce the amount of excess soluble EGFP-Rab. (vi) The final membrane fraction was then resuspended by brief sonication and the concentration of EGFP-Rab determined based on the EGFP fluorescence in reference to purified Slp1(aa1-116)-EGFP. (B) (i) EGFP-Rab:GDI complexes were formed by extraction of the Rab proteins from the membrane fractions with GDI $\alpha$ . The membrane fraction containing the EGFP-Rab was incubated with GDI, followed by ultracentrifugation to separate the membranes from the solubilized EGFP-Rab. (ii) The resulting membrane pellet was re-solubilized by sonication and (iii) the fluorescence of the membrane fraction and the complex containing supernatant (SN) was compared to determine the yield of the complex. (C) The EGFP-Rab:GDI complex was used in membrane delivery assays. (i) Large vesicles were incubated with the complex and (ii) streptavidin was added to enhance pelleting of the membranes in the following ultracentrifugation step. (iii) The supernatant was then removed and the membrane pellet resuspended in SDS-loading buffer. (iv) The amount of EGFP-Rab in both fractions and the percentage of Rab membrane recruitment was analysed by Western blotting and densitometry. This Figure is reproduced in color in *Molecular Membrane Biology* online.

membrane, in particular the levels of stored curvature elastic stress therein, contribute to controlling this equilibrium.

## Methods

### General outline of the Rab membrane delivery assay

EGFP-Rabs proteins overexpressed in HEK293 cells were employed to facilitate reproducible and comparable measurements with different Rab family members and to solve issues associated with long-term storage of Rab:GDI complexes. The approach is illustrated in Figure 2. For the preparation of the EGFP-Rab membrane fraction (see Figure 2A), EGFP-Rab proteins were overexpressed in HEK293A cells. Cells were lysed 48 h post-transfection by sonication and the post-nuclear supernatant (PNS)

prepared by centrifugation of the total lysate to remove large debris and genomic DNA. Membrane fractions were then prepared by ultracentrifugation of the PNS. The resulting membrane pellet was sonicated in fresh buffer and pelleted again by another step of ultracentrifugation, followed by sonication of the membrane pellet in fresh buffer. This additional purification step of the membrane fraction was crucial as it removed loosely associated EGFP-Rab protein from the membrane fraction and markedly improved the quality of the subsequent Rab:GDI complex formation. The Rab concentration in the membrane fraction was determined by measuring the EGFP fluorescence and correlating it to an EGFP standard curve generated using purified Slp1(aa1-116)-EGFP (obtained from A. N. Hume and A. K. Tarafder).

For Rab:GDI complex formation (see Figure 2B) membrane fractions containing 0.6  $\mu$ M overexpressed

Rab protein were incubated with 1  $\mu$ M GDI for 30 min at 37°C, followed by ultracentrifugation to separate the membranes from the supernatant containing the soluble EGFP-Rab:GDI complex. The resulting membrane pellet, containing the remaining EGFP-Rab was resuspended by sonication in fresh buffer and the Rab:GDI complex concentration was determined by measuring the EGFP fluorescence of the soluble and membrane fractions. Further purification of the complex by NiNTA affinity purification or gel filtration severely interfered with complex stability and was considered not necessary due to the relative purity obtained after Rab extraction from membranes.

Large vesicles of different lipid compositions were formed by extrusion and used in Rab membrane delivery assays (see Figure 2C). To enhance pelleting of the membranes 1% biotinylated DOPE (Biotinyl Cap PE (BCPE) or 1,2-dioleoyl-*sn*-glycero-3-phosphoethanolamine-N-(cap biotinyl)) was incorporated into the vesicles. During incubation of the vesicles with the EGFP-Rab:GDI complex streptavidin was added to the samples in order to enhance pelleting of the membranes during the following ultracentrifugation. Equivalent volumes of the supernatant and membrane fraction were then analysed by SDS-PAGE followed by immunoblotting to quantify Rab membrane partitioning.

#### *Preparation of recombinant GDI $\alpha$ and $\beta$ from Sf9 cells*

N-terminally his-tagged human GDI $\alpha$  and  $\beta$  isoforms were subcloned into pFastBacHtb vectors (Invitrogen, Paisley, Scotland, UK) and recombinant baculovirus was produced according to the Bac-to-Bac baculovirus expression system (Invitrogen) in Sf9 cells. 500 ml Sf9 culture was harvested 48 h post-infection and lysed in 30 ml lysis buffer (50 mM Tris, pH 7.5; 150 mM NaCl; 5 mM MgCl<sub>2</sub>; 1 mM  $\beta$ -mercaptoethanol; 0.2% Triton X-100; 1  $\times$  Complete protease inhibitor cocktail (PI) (Roche Applied Science, Burgess Hill, UK). The total lysate was then centrifuged for 1 h at 100,000 *g* at 4°C. The supernatant fraction (S100) of the total lysate was added to 5 ml NiNTA beads equilibrated in lysis buffer without PI and incubated for 2–3 h at 4°C under gentle end over end agitation. NiNTA beads were harvested by centrifugation at 4000 *g*, 4°C for 10 min and washed once in 50 ml lysis buffer (without PI) and twice in lysis buffer with 0.2% (w/v) CHAPS instead of Triton X-100. The beads were transferred into a column and bound proteins were eluted with a stepwise gradient of imidazole

in lysis buffer (+0.2% (w/v) CHAPS) from 10–200 mM. Eluted fractions were analysed by SDS-PAGE followed by Coomassie staining. Fractions containing the protein of interest were pooled and concentrated using 30 kDa cut-off Vivaspin columns (GE Healthcare, Chalfont St Giles, Buckinghamshire, UK) to a concentration of 1–3 mg/ml followed by buffer exchange on a PD10 column (Pierce, Thermo Fisher Scientific, Rockford, IL, USA) to 50 mM Tris pH 7.5, 150 mM NaCl, 5 mM MgCl<sub>2</sub>, 1 mM  $\beta$ -mercaptoethanol, 0.2% CHAPS. The fractions were pooled and concentrated again to 1–3 mg/ml.

#### *Cell culture*

All cell culture media were obtained from Gibco (Invitrogen). HEK293A cells were cultured in Dulbecco's Eagle Modified Medium (DMEM) supplemented with 10% fetal bovine serum (FBS), 100 U/ml penicillin and 100 U/ml streptomycin at 10% CO<sub>2</sub> and 37°C. 10 cm dishes were transfected with various EGFP-Rab constructs at 70–80% confluency using FuGENE6 (Roche Applied Science). Cells were harvested 48 h post-transfection by scraping in ice cold phosphate buffered saline (PBS) and washing once in 10 ml ice cold PBS.

#### *Preparation of EGFP-Rab membrane fractions*

For preparation of HEK293A P100 membrane fractions containing EGFP-Rab, cell pellets derived from one 10 cm dish were lysed in 750  $\mu$ l lysis buffer (50 mM Tris, pH 7.5; 150 mM NaCl; 5 mM MgCl<sub>2</sub>; 1 mM dithioerythritol (DTE); 1  $\times$  Complete protease inhibitor cocktail (PI) (Roche Applied Science) by vortexing, followed by 30 s sonication at 5  $\mu$ m amplitude with a titanium tip sonicator (MSE Soniprep 150, London, UK). The post-nuclear supernatant (PNS) was prepared by centrifugation of the total lysate at 2000 *g* for 5 min at 4°C. From the resulting supernatant the cellular membranes were purified by ultracentrifugation at 100,000 *g* at 4°C for 45 min. The supernatant was discarded and the membrane pellet re-solubilized in 750  $\mu$ l extraction buffer (50 mM HEPES pH 7.2; 150 mM NaCl; 5 mM MgCl<sub>2</sub>; 1 mM DTE; 1  $\times$  PI) by 30 s sonication as above. To remove soluble EGFP-Rab non-specifically associated with the membrane fraction, the membranes were again recovered by the same ultracentrifugation step. The resulting P100 membrane fraction was sonicated again in 750  $\mu$ l extraction buffer for 30 s at 5  $\mu$ m to solubilize the membranes.



### EGFP-Rab GDI extraction from HEK293A membrane fractions

The fluorescence emission at 509 nm of washed P100 fractions containing EGFP-Rab proteins was quantified ( $\lambda_{\text{ex}} = 488$  nm) based on EGFP fluorescence using a standard curve of purified Slp1(aal-116)-EGFP. Slp1 is a cytosolic Rab27 effector and its N-terminus does not interact with membranes (McAdara Berkowitz et al. 2001, Catz et al. 2002, Strom et al. 2002). The optimal amount of GDI required for preparative Rab:GDI complex formation was determined by a titration range of increasing amounts of GDI. It was important to maximize the complex yield while minimizing the amount of free GDI in the resulting complex samples, as any excess GDI in the sample shifts the equilibrium of Rab-membrane binding to Rab-GDI association. For this reason EGFP-Rab membrane fractions containing 0.6  $\mu\text{M}$  EGFP-Rab were mixed with GDI at final concentrations of 0/0.1/0.2/0.5/1.0/2.0  $\mu\text{M}$  in a total volume of 50  $\mu\text{l}$  and incubated at 37°C for 20 min. The tubes were immediately transferred to a pre-cooled TLA45 rotor (Beckman Coulter, High Wycombe, UK) and centrifuged at 100,000  $g$  for 30 min at 4°C. The supernatant was removed and the pellet resuspended in 50  $\mu\text{l}$  extraction buffer (see above) in a water bath sonicator for 10 min at room temperature. The complete volume of the soluble (S100) and membrane (P100) fractions were transferred into a white flat bottom NSB 384-well plate (Corning, Amsterdam, The Netherlands) and the fluorescence emission was quantified ( $\lambda_{\text{ex}} = 488$  nm,  $\lambda_{\text{em}} = 509$  nm) using a fluorescence spectrophotometer (Varian, Cary Eclipse, Walton-on-Thames, Surrey, UK). The background fluorescence of the buffer was measured and subtracted from each sample and the proportion of EGFP-Rab present in the supernatant fraction was calculated.

For preparative Rab:GDI complex formation Rab extraction from HEK293A membrane fractions was scaled up (see Figure 2B). Extraction was performed with 1  $\mu\text{M}$  GDI $\alpha$  or  $\beta$  and 0.6  $\mu\text{M}$  EGFP-Rab in typical volumes of 1 ml for 30 min at 37°C, followed by ultracentrifugation at 100,000  $g$  for 45 min at 4°C. The resulting supernatant contains the EGFP-Rab:GDI complex, which was kept on ice and used within 24 h of preparation. Control samples without GDI were used in parallel to determine the amount of soluble-free EGFP-Rab in the supernatant.

### Vesicle preparation

Lipids (1,2-dioleoyl-*sn*-glycero-3-phosphocholine (DOPC), 1,2-dioleoyl-*sn*-glycero-3-phosphoethanolamine

(DOPE), 1,2-dimyristoyl-*sn*-glycero-3-phosphocholine (DMPC), and 1,2-di-(9Z-octadecenoyl)-*sn*-glycero-3-phosphoethanolamine-N-(cap biotinyl) (BCPE) were purchased from Avanti Polar Lipids (Alabaster, AL, USA). Stocks were prepared by dissolving powdered lipids in cyclohexane, lyophilization overnight and addition of  $\text{CHCl}_3/\text{MeOH}$  3:1 to the desired stock concentration. For vesicle preparation, lipids in solvent were mixed and dried under nitrogen stream to remove the majority of solvent, followed by removal of residual solvent overnight under vacuum. Buffer (50 mM HEPES pH 7.2; 150 mM NaCl; 5 mM  $\text{MgCl}_2$ ) was then added to a final lipid concentration of 2 mM and the lipid suspension subjected to five freeze-thaw-vortex cycles. Large vesicles were produced by extruding the lipid suspension  $19 \times$  through 0.4  $\mu\text{m}$  pore size polycarbonate filters (Avanti Polar Lipids), using the Mini-Extruder from Avanti Polar Lipids.

### Rab membrane-delivery assays

Vesicles were mixed with EGFP-Rab:GDI complex at final concentrations of 0.25 mM lipid and 0.25  $\mu\text{M}$  Rab:GDI and incubated at 37°C for 15 min. Streptavidin (Sigma Aldrich, Gillingham, Kent, UK) was added to a final concentration of 0.4  $\mu\text{M}$  followed by further incubation at 37°C for 15 min and 10 min at room temperature to enhance pelleting of the membranes (Tortorella et al. 1993). The samples were then centrifuged for 1 h at 180,000  $g$  at 4°C, followed by removal of the supernatant and resuspension of the pellet in the equivalent volume of the supernatant with extraction buffer (see Figure 2C).

## Results

In the cell, Rab GTPases are delivered from the cytosol to their target membranes by GDI (Ullrich et al. 1993, 1994). Therefore, the first step toward investigating Rab membrane recruitment was forming high quantities of the stable binary Rab:GDI complex. In initial experiments the complex stability proved to be too low for freezing (data not shown) and accordingly Rab:GDI complex was prepared freshly for each independent set of experiments. EGFP-tagged Rab proteins were used as the EGFP fluorescence allows reliable quantification of the complex in solution. Consequently, the complex concentration used in membrane binding experiments could be adjusted precisely, facilitating comparisons between independent experiments and different Rab family members. Using unlabelled

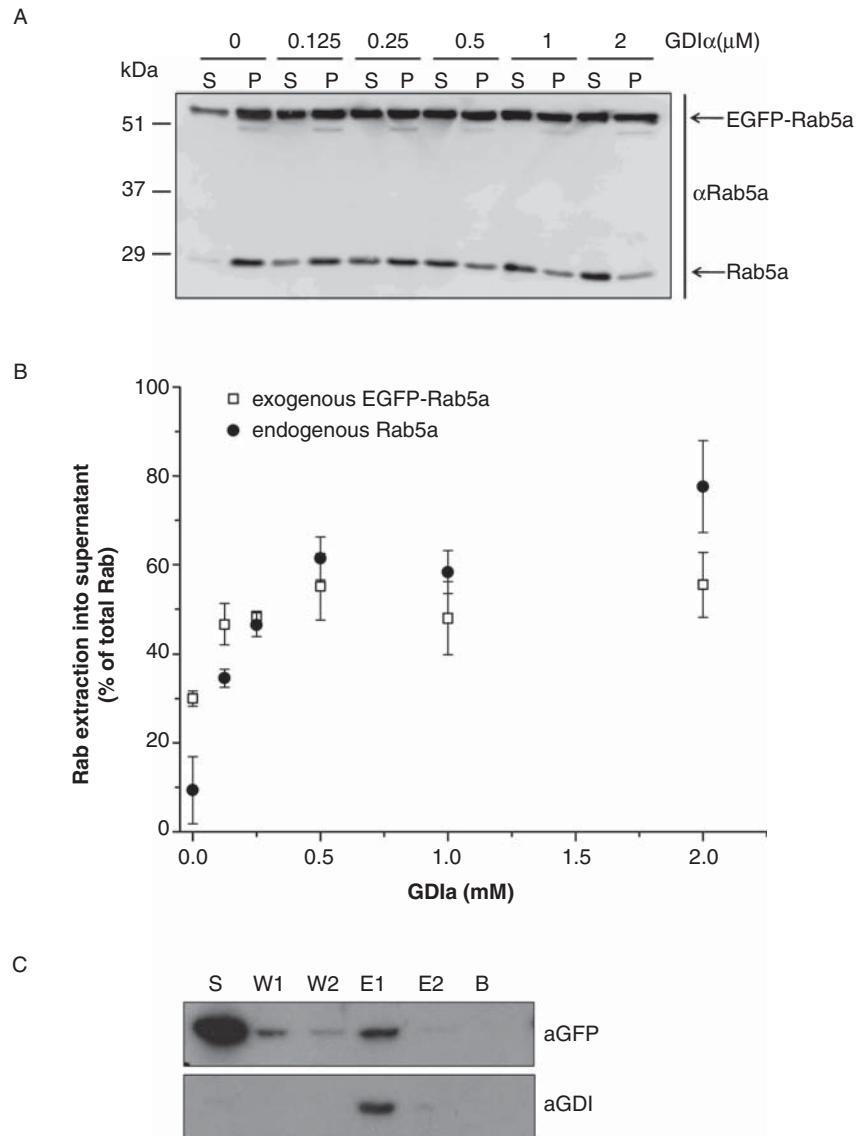


Figure 3. Validation of EGFP-Rab:GDI complex formation. (A) Exemplary Western blot of extraction of endogeneous Rab5a and overexpressed EGFP-Rab5a with increasing amounts of GDI $\alpha$  (0–2  $\mu$ M) from HEK293A membrane fractions showing the supernatant (S) and membrane (P) fractions, probed with  $\alpha$ Rab5a antibody. (B) Quantification of extraction by densitometry. (C) EGFP-Rab1a:GDI $\beta$  co-precipitation. After EGFP-Rab1a extraction from HEK293A membrane fraction with 1  $\mu$ M GDI $\beta$ , his-tagged GDI $\beta$  was affinity purified using NiNTA beads. (S, Supernatant of beads; W1/W2, Wash fractions using 250  $\mu$ l elution buffer; E1/E2, Elution fractions using 250  $\mu$ l elution buffer containing 200 mM imidazole; B, beads).

Rab proteins would only permit indirect quantification of the complex, for example by Western blotting, which would be more time-consuming and for this reason may also be problematic in terms of the complex stability, as Rab:GDI complex was used for membrane delivery experiments immediately after complex formation.

Endogenous Rab5a and EGFP-tagged overexpressed Rab5a are extracted from HEK293A membranes into the soluble fraction by GDI $\alpha$  in a comparable manner, validating the use of EGFP-

tagged Rab proteins for Rab membrane-binding studies (Figure 3A and B). Complex existence in the supernatant fraction after extraction with his-tagged GDI $\alpha$  was confirmed by pulling down GDI onto NiNTA resin. Figure 3C shows that EGFP-Rab5a co-elutes from beads in the same fraction as GDI $\alpha$ , indicating that complex formation in the previous extraction step was successful.

To optimize extraction conditions and minimize the presence of excess free GDI in the Rab:GDI complex samples, Rab membrane extractions were

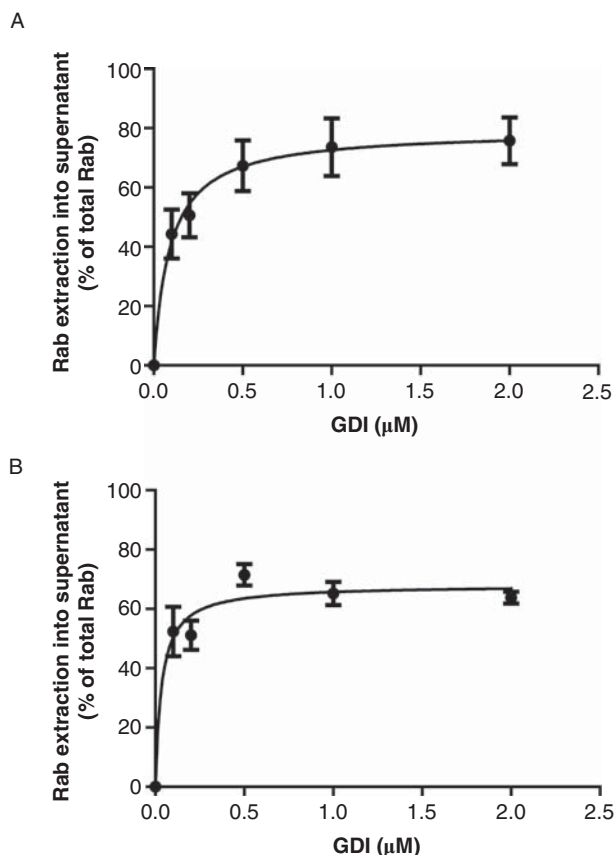


Figure 4. Extraction of (A) EGFP-Rab1a and (B) EGFP-Rab5a from HEK293A membrane fractions into the soluble fraction with increasing amount of GDI $\alpha$ . Freshly prepared EGFP-Rab membrane fractions containing 0.6  $\mu$ M EGFP-Rab were incubated with the indicated concentrations of GDI, followed by separation of the membrane and soluble fractions by ultracentrifugation and quantification of the EGFP fluorescence of both fractions. The percentage of extracted Rab is given by the ratio of the EGFP fluorescence in the supernatant and the total EGFP fluorescence of both fractions.

performed with the concentration of GDI ranging between 0 and 2  $\mu$ M. This leads to extraction curves as shown in Figure 4 for Rab1a and Rab5a, revealing that both Rab proteins are extracted to around 60–70%, reaching saturation at around 0.5 mM GDI.

After complex formation, the EGFP-fluorescence was used to determine the Rab:GDI concentration and to dilute each complex sample to a common concentration used in subsequent membrane delivery assays. To investigate the influence of the lipid composition on Rab recruitment simple well-established lipid mixtures were employed. This allowed direct correlation of the membrane properties to Rab recruitment.

Unfortunately, the EGFP fluorescence of the Rab-fusion proteins could not be used to quantify Rab membrane partitioning due to very inconsistent data (not shown). This was probably due to a combination

of low signals and the fact that the lipid vesicles produced by sonication scattered and quenched the fluorescence. However, attempts to solubilize the vesicles with detergent in order to recover the fluorescence signals were also unsuccessful. Therefore, the Rab content of the resulting membrane and soluble fractions were analyzed by Western blotting (see Figure 5A and Supplementary Figure S3, available online), as were the controls (Supplementary Figures S1 and S2, available online) and the percentage of membrane binding was quantified by densitometry of the EGFP-Rab signals.

To determine the optimal amount of lipids used in Rab membrane delivery assays, a fixed amount of complex (0.25  $\mu$ M) was incubated with increasing concentrations of binary membrane mixtures consisting of DOPC:DOPE 9:1 (0/0.125/0.25/0.5/1.0/2.0 mM), leading to a saturation curve as shown in Figure 5A and B. When too much lipid is used in the membrane delivery assays, differential Rab binding to different membrane compositions will be masked. Any difference in membrane preference of Rab proteins will be expected to be most pronounced in the pre-saturated region between around 0 and 1 mM lipid. However, if the lipid concentration is too low, the measurement of Rab membrane binding may become problematic in terms of sensitivity and accuracy. With these considerations in mind and using the data shown in Figure 5, 0.25 mM lipid was used in subsequent Rab membrane delivery assays, corresponding to a lipid/Rab protein ratio of 1000. Concluding from the data set in Figure 5, this ratio is below the saturation threshold of the membranes with Rab protein and suitable for reliable detection of membrane association of Rab proteins.

The addition of DOPC to DMPC or DOPE to DOPC monotonically increases Rab5a binding (Figure 6A). The corresponding Western blots are shown in Supplementary Figure S3 (available online). As a negative control membrane binding of Slp1 (aa1-116)-EGFP was shown not to bind to membranes at all (Supplementary Figure S1, online) and neither did GDI (Supplementary Figure S2), confirming that the EGFP-Rab membrane association is Rab specific. 30% of Rab5a is found to be membrane bound in DOPC:DMPC 6:4 (molar ratio) vesicles, increasing to 50% in DOPC:DOPE 6:4 systems. This overall trend of increasing membrane binding was confirmed with Rab1a, as shown in Figure 5B, suggesting that this selectivity in membrane binding may be a general feature of Rab GTPases. Around 27% binding of Rab1a to DOPC:DMPC 6:4 was observed, increasing to 57% for DOPC:DOPE 6:4.



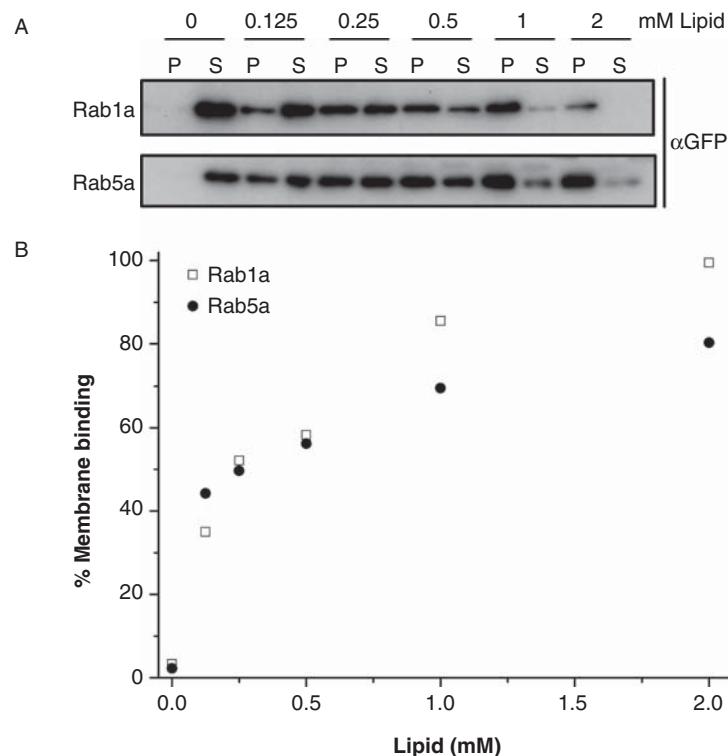


Figure 5. Membrane delivery of EGFP-Rab1a and EGFP-Rab5a using increasing concentration of lipids (0–2 mM). 0.25  $\mu$ M EGFP-Rab:GDI complex was incubated with the indicated concentration of lipid vesicles composed of DOPC:DOPE 8:2, containing 1% Biotinyl-Cap-PE. 0.4  $\mu$ M Streptavidin was added to the mixtures to enhance pelleting of the vesicles by ultracentrifugation. (A) Exemplary Western blots of EGFP-Rab1a and EGFP-Rab5a partitioning between supernatant (S) and membrane (P) fractions with increasing concentration of lipid. (B) Densitometry analysis of Western blots shows the percentage of membrane associated Rab protein and the corresponding membrane saturation curve.

## Discussion

Our experiments demonstrate for the first time that Rab binding to membranes is sensitive to the lipid environment. In order to interpret the Rab-membrane binding results and understand the specific biophysical property of the bilayer that regulates association with membranes containing a diverse mixture of phospholipids, we must consider the local intermolecular forces between lipids in a membrane (Shearman et al. 2006). Electrostatic interactions are often used to account for differences in membrane-protein interactions but throughout our assay, the choice of zwitterionic lipids eliminates these as regulating factors. In addition, both the DMPC/DOPC and DOPC/DOPE binary systems have previously been studied and shown not to exhibit phase separation or changes in the distribution of vesicle diameters over the composition regimes of our studies (Attard et al. 2000). This excludes gross inhomogeneities and geometrical curvature effects as the source of the variation in Rab localization. The data are also inconsistent with Rab binding depending on molecular area as the average value of cross sectional area

per molecule (A) increases from 67  $\text{\AA}^2$  for 100 mol% DMPC to 76  $\text{\AA}^2$  for 100 mol% DOPC (Costigan et al. 2000) before dropping to approximately 69  $\text{\AA}^2$  at 60 mol% DOPE (Kozlov et al. 1994) due to the lower hydrophilicity of the phosphatidylethanolamine headgroup (Templer et al. 1998).

By contrast, the lipid mixtures selected do vary in terms of their ability to alter the curvature of the lipid-water interface. In general, type I lipids are characterized by their ability to form molecular aggregates in which the polar/apolar interface curves away from the polar environment whereas type II lipids exhibit interfaces which curve towards the polar environment (Chernomordik and Kozlov 2003). When we examine a monolayer and sum up all the pressures  $\pi(z)$  acting across it we obtain the net lateral stress which for a monolayer at equilibrium is zero:

$$\int \pi(z) dz = 0 \quad (1)$$

The torque acting on the monolayer is given by the first moment of the stress profile which in general is non-zero:

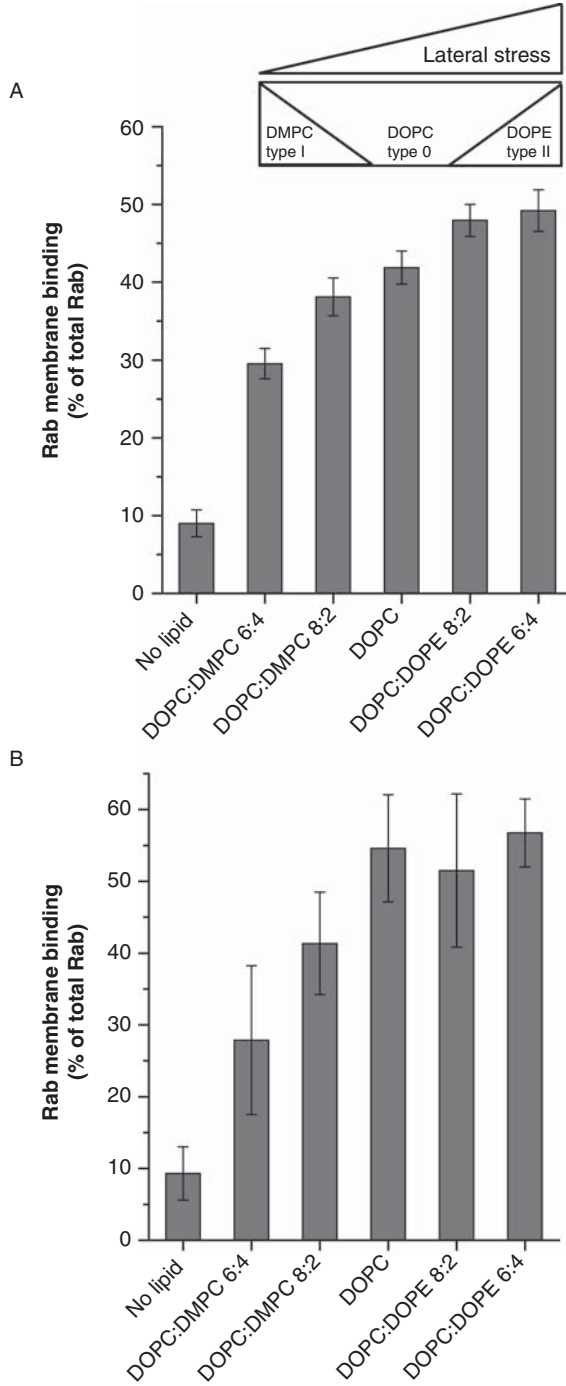


Figure 6. Membrane binding of (A) EGFP-Rab5a and (B) EGFP-Rab1a to vesicles of different lipid compositions. Large vesicles were produced by extrusion of a 2 mM suspension through a 400 nm pore size membrane. Supernatant and membrane fraction were analysed by Western blotting to determine the percentage of membrane partitioning of each Rab by densitometry. The lipid free control shows the amount of non-specific Rab binding to the tube walls. The data is derived from five (Rab5a) or four (Rab1a) separate sets of measurements, each performed in at least duplicates. Error bars represent mean  $\pm$  SE (standard error).

$$\tau = -\int \pi(z)zdz = -2\kappa c_0 \quad (2)$$

where  $\tau$  is the torque tension and is the torque stored in a monolayer when it is constrained to remain flat,  $\kappa$  is the bending rigidity of the monolayer, and  $c_0$  is the spontaneous curvature of the monolayer. For a monolayer to be stable there should be zero net torque exerted about the neutral surface of the monolayer. If this is not the case and we instead have a situation in which there is an imbalance in the forces exerted in the headgroup and chain regions, a net monolayer torque tension will be applied to the monolayer, the direction of which will depend on which set of forces is greatest. The monolayer will wish to curve away from or towards the water but such a situation is problematic because of the back to back arrangement of the monolayers in a bilayer.

A useful way to quantify the torque tension is via the Helfrich Hamiltonian (Equation 3) for the stored curvature elastic energy per amphiphile in a monolayer:

$$g_C = 1/2\kappa A(c_1 + c_2 - 2c_0)^2 + \kappa_G A c_1 c_2 \quad (3)$$

where  $A$  is the cross-sectional area per molecule,  $c_1$  and  $c_2$  are the principal curvatures at the interface, and  $\kappa_G$  the Gaussian curvature modulus. The torque tension of the monolayer is related to the curvature elastic parameters via (Equation 2), namely that  $\tau = -2\kappa c_0$ . For multicomponent lipid systems that mix homogeneously, it is therefore possible to determine the torque tension from a knowledge of the effective values of  $c_0$  and the bending rigidities of the monolayer. These values can also be used to find the stored curvature elastic energy per molecule (Equation 4) stored in a flat monolayer relative to the spherical geometry of a monolayer in which no torque is manifested, namely:

$$g_C = 2\kappa A c_0^2 (1 - \kappa_G (2\kappa + \kappa_G)) \quad (4)$$

In our experiments the spontaneous curvature changes monotonically from DMPC to DOPC to DOPE and according to (Equations 3 and 4) so too do the torque tension and stored curvature elastic energy. Upon increasing the amount of DOPC in DMPC/DOPC mixtures, the presence of *cis*-unsaturated acyl chains and chain unsaturation leads to an increase in the degree of acyl chain splay and desire for curvature towards the water. In turn, this leads to a rise in the torque tension and stored curvature elastic energy. As we increase the amount of DOPE in DOPC/DOPE systems (chain type is invariant) a further rise in the torque tension ensues driven by

the lower hydrophilicity of the phosphatidylethanolamine headgroup which imparts a greater desire for curvature towards the polar region relative to DOPC.

As the stored curvature elastic energy and torque tension increases monotonically from DMPC to DOPC to DOPE so too does the degree of Rab binding to the membrane. The activity and binding of other peripheral proteins such as CCT have also been shown to correlate with the stored curvature elastic energy in the membrane (Attard et al. 2000). The mode of action is one in which insertion of the protein into the membrane interface allows the chains of nearby lipids to splay. This leads to a reduction in the free energy of the system via a favourable reduction in the stored curvature elastic energy. Similarly in our experiments, as the amount of type II lipids in the membrane increases the equilibrium between free and bound Rab shifts towards the bound state in order to relieve the stored curvature elastic energy.

The simplified binary membrane systems used in this work cannot be compared to the complexity of cellular membranes and therefore we do not attempt to explain the mechanism how Rab proteins target different membrane *in vivo*. In addition, physical properties of complex lipid mixtures are still not well described and therefore no correlation between the lipid mixtures used here and the preferred membranes of Rab1a (ER and Golgi apparatus) and Rab5a (plasma membrane and endocytic vesicles) can be made. However, this work provides the first evidence for Rab proteins in general being able to differentiate between membranes with different physical properties in the absence of other protein factors.

## Conclusions

Our study addresses a number of open questions in the Rab field, including Rab:GDI extraction and Rab recycling and a contributory factor towards directed Rab membrane targeting. The assay developed in these studies opens up the possibility of being able to investigate Rab membrane targeting under a range of conditions. We also report a reproducible and quick method for producing EGFP-Rab:GDI complexes. Due to the EGFP-tag, assay conditions can be normalized between different sets of experiments. This allows investigation of Rab extraction from membranes by GDI as well as delivery of Rab by GDI to membranes. Using simple binary lipid mixtures with well-established biophysical properties we have shown there is a strong correlation between Rab binding and lipid composition via sensing of the torque tension and stored curvature elastic energy. Membrane binding to the artificial membrane model

systems used in this study occurred in the absence of further targeting factors which have been suggested to facilitate Rab membrane recruitment and binding *in vivo* (Sivars et al. 2003, Aivazian et al. 2006, Tarafder et al. 2011). In addition, GDI $\alpha$  dissociates off the complex and is not detected on the membranes (Supplementary Figure S2), demonstrating that in this experimental set-up no protein GDFs were required for stable Rab membrane association, notably in the absence of GTP. These findings indicate that the lipid composition of membranes may act as an additional targeting factor for Rab membrane recruitment.

## Acknowledgements

Purified Slp1(aa1-116)-EGFP was obtained from Alistair Hume and Abul Tarafder, pEGFP-mRab constructs were obtained from José Ramalho (New University of Lisbon). This work was supported by ESPRC Platform grant EP/J017566/1, and by an EPSRC Centre for Doctoral Training Studentship from the Institute of Chemical Biology Centre for Doctoral Training awarded to MK.

**Declaration of interest:** The authors report no conflicts of interest. The authors alone are responsible for the content and writing of the paper.

## References

- Aivazian D, Serrano RL, Pfeffer S. 2006. TIP47 is a key effector for Rab9 localization. *J Cell Biol* 173:917–926.
- Akavia UD, Litvin O, Kim J, Sanchez-Garcia F, Kotliar D, Causton HC, et al. 2010. An integrated approach to uncover drivers of cancer. *Cell* 143:1005–1017.
- Alexandrov K, Simon I, Iakovenko A, Holz B, Goody RS, Scheidig AJ. 1998. Moderate discrimination of REP-1 between Rab7  $\times$  GDP and Rab7  $\times$  GTP arises from a difference of an order of magnitude in dissociation rates. *FEBS Lett* 425:460–464.
- Ali BR, Wasmeier C, Lamoreux L, Strom M, Seabra MC. 2004. Multiple regions contribute to membrane targeting of Rab GTPases. *J Cell Sci* 117:6401–6412.
- Attard GS, Smith WS, Templer RH, Hunt AN, Jackowski S. 1998. Modulation of CTP:phosphocholine cytidyltransferase by membrane torque tension. *Biochem Soc Trans* 26:S230.
- Attard GS, Templer RH, Smith WS, Hunt AN, Jackowski S. 2000. Modulation of CTP:phosphocholine cytidyltransferase by membrane curvature elastic stress. *PNAS* 97:9032–9036.
- Barral DC, Ramalho JS, Anders R, Hume AN, Knapton HJ, Tolmachova T, et al. 2002. Functional redundancy of Rab27 proteins and the pathogenesis of Griscelli syndrome. *J Clin Invest* 110:247–257.
- Beck R, Sun Z, Adolf F, Rutz C, Bassler J, Wild K, et al. 2008. Membrane curvature induced by Arf1-GTP is essential for vesicle formation. *PNAS* 105:11731–11736.

- Bigay J, Casella J-F, Drin G, Mesmin B, Antonny B. 2005. ArfGAP1 responds to membrane curvature through the folding of a lipid packing sensor motif. *Embo J* 24:2244–2253.
- Booth PJ. 2000. Unravelling the folding of bacteriorhodopsin. *Biochim Biophys Acta* 1460:4–14.
- Booth PJ, Clarke J. 2010. Membrane protein folding makes the transition. *PNAS* 107:3947–3948.
- Catz SD, Johnson JL, Babior BM. 2002. The C2A domain of JFC1 binds to 3'-phosphorylated phosphoinositides and directs plasma membrane association in living cells. *PNAS* 99:11652–11657.
- Charalambous K, Miller D, Curnow P, Booth PJ. 2008. Lipid bilayer composition influences small multidrug transporters. *BMC Biochem* 9:31.
- Chernomordik LV, Kozlov MM. 2003. Protein-lipid interplay in fusion and fission of biological membranes. *Annu Rev Biochem* 72:175–207.
- Costigan SC, Booth PJ, Templer RH. 2000. Estimations of lipid bilayer geometry in fluid lamellar phases. *Biochim Biophys Acta* 1468:41–54.
- Curnow P, Lorch M, Charalambous K, Booth PJ. 2004. The reconstitution and activity of the small multidrug transporter EmrE is modulated by non-bilayer lipid composition. *J Mol Biol* 343:213–222.
- Dirac-Svejstrup AB, Sumizawa T, Pfeffer SR. 1997. Identification of a GDI displacement factor that releases endosomal Rab GTPases from Rab-GDI. *Embo J* 16:465–472.
- Ganley IG, Pfeffer SR. 2006. Cholesterol accumulation sequesters Rab9 and disrupts late endosome function in NPC1-deficient cells. *J Biol Chem* 281:17890–17899.
- Hendrix A, Maynard D, Pauwels P, Braems G, Denys H, Van den Broecke R, et al. 2010. Effect of the secretory small GTPase Rab27B on breast cancer growth, invasion, and metastasis. *J Natl Cancer Inst* 102:866–880.
- Hong H, Tamm LK. 2004. Elastic coupling of integral membrane protein stability to lipid bilayer forces. *PNAS* 101:4065–4070.
- Horiuchi H, Ullrich O, Bucci C, Zerial M. 1995. Purification of posttranslationally modified and unmodified Rab5 protein expressed in *Spodoptera frugiperda* cells. *Meth Enzymol* 257:9–15.
- Hutagalung AH, Novick PJ. 2011. Role of rab GTPases in membrane traffic and cell physiology. *Physiol Rev* 91:119–149.
- Jancic C, Savina A, Wasmeier C, Tolmachova T, El-Benna J, Dang PM-C, et al. 2007. Rab27a regulates phagosomal pH and NADPH oxidase recruitment to dendritic cell phagosomes. *Nat Cell Biol* 9:367–378.
- Johnson JL, Brzezinska AA, Tolmachova T, Munafo DB, Ellis BA, Seabra MC, et al. 2010. Rab27a and Rab27b regulate neutrophil azurophilic granule exocytosis and NADPH oxidase activity by independent mechanisms. *Traffic* 11:533–547.
- Kozlov MM, Leikin S, Rand RP. 1994. Bending, hydration and interstitial energies quantitatively account for the hexagonal-lamellar-hexagonal reentrant phase transition in dioleoylphosphatidylethanolamine. *Biophys J* 67:1603–1611.
- Lee MCS, Orci L, Hamamoto S, Futai E, Ravazzola M, Schekman R. 2005. Sar1p N-terminal helix initiates membrane curvature and completes the fission of a COPII vesicle. *Cell* 122:605–617.
- Lewis JR, Cafiso DS. 1999. Correlation between the free energy of a channel-forming voltage-gated peptide and the spontaneous curvature of bilayer lipids. *Biochemistry* 38:5932–5938.
- Lipinski AR, Heymann J, Meissner C, Karlas A, Brinkmann V, Meyer TF, et al. 2009. Rab6 and Rab11 regulate chlamydia trachomatis development and Golgin-84-dependent Golgi fragmentation. *PLoS Pathogens* 5:12.
- Lipowsky R. 1991. The conformation of membranes. *Nature* 349:475–481.
- Lombardi D, Soldati T, Riederer MA, Goda Y, Zerial M, Pfeffer SR. 1993. Rab9 functions in transport between late endosomes and the trans Golgi network. *Embo J* 12:677–682.
- Machner MP, Isberg RR. 2007. A bifunctional bacterial protein links GDI displacement to Rab1 activation. *Science* 318:974–977.
- Marsh D. 2006. Elastic curvature constants of lipid monolayers and bilayers. *Chem Phys Lipids* 144:146–159.
- McAdara Berkowitz JK, Catz SD, Johnson JL, Ruedi JM, Thon V, Babior BM. 2001. JFC1, a novel tandem C2 domain-containing protein associated with the leukocyte NADPH oxidase. *J Biol Chem* 276:18855–18862.
- Miller D, Charalambous K, Rotem D, Schuldiner S, Curnow P, Booth PJ. 2009. In vitro unfolding and refolding of the small multidrug transporter EmrE. *J Mol Biol* 393:815–832.
- Mizuno K, Tolmachova T, Ushakov DS, Romao M, Abrink M, Ferenczi MA, et al. 2007. Rab27b regulates mast cell granule dynamics and secretion. *Traffic* 8:883–892.
- Nagy JK, Lonzer WL, Sanders CR. 2001. Kinetic study of folding and misfolding of diacylglycerol kinase in model membranes. *Biochemistry* 40:8971–8980.
- Nishimura N, Nakamura H, Takais Y. 1994. Molecular cloning and characterization of two rab GDI species from rat brain: Brain-specific and ubiquitous types. *Biochemistry* 269:14191–14198.
- Pereira-Leal JB, Seabra MC. 2000. The mammalian Rab family of small GTPases: Definition of family and subfamily sequence motifs suggests a mechanism for functional specificity in the Ras superfamily. *J Mol Biol* 301:1077–1087.
- Pereira-Leal JB, Seabra MC. 2001. Evolution of the Rab family of small GTP-binding proteins. *J Mol Biol* 313:889–901.
- Pfeffer S. 2005. A model for Rab GTPase localization. *Biochem Soc Trans* 33:627–630.
- Pfeffer S, Aivazian D. 2004. Targeting Rab GTPases to distinct membrane compartments. *Nat Rev Mol Cell Biol* 5:886–896.
- Seabra MC, Brown MS, Goldstein JL. 1993. Retinal degeneration in choroideremia: Deficiency of rab geranylgeranyl transferase. *Science* 259:377–381.
- Seabra MC, Wasmeier C. 2004. Controlling the location and activation of Rab GTPases. *Curr Opin Cell Biol* 16:451–457.
- Seddon AM, Lorch M, Ces O, Templer RH, Macrae F, Booth PJ. 2008. Phosphatidylglycerol lipids enhance folding of an alpha helical membrane protein. *J Mol Biol* 380:548–556.
- Shapiro AD, Pfeffer SR. 1995. Quantitative analysis of the interactions between prenyl Rab9, GDP dissociation inhibitor-alpha, and guanine nucleotides. *J Biol Chem* 270:11085–11090.
- Shearman GC, Ces O, Templer RH, Seddon JM. 2006. Inverse lyotropic phases of lipids and membrane curvature. *J Phys Condens Matter* 18:S1105–S1124.
- Sivars U, Aivazian D, Pfeffer SR. 2003. Yip3 catalyses the dissociation of endosomal Rab-GDI complexes. *Nature* 425:856–859.
- Soldati T, Shapiro AD, Svejstrup AB, Pfeffer SR. 1994. Membrane targeting of the small GTPase Rab9 is accompanied by nucleotide exchange. *Nature* 369:76–78.
- Strom M, Hume AN, Tarafder AK, Barkagianni E, Seabra MC. 2002. A family of Rab27-binding proteins. Melanophilin links Rab27a and myosin Va function in melanosome transport. *J Biol Chem* 277:25423–25430.
- Tarafder AK, Wasmeier C, Figueiredo AC, Booth AEG, Orihara A, Ramalho JS, et al. 2011. Rab27a targeting to melanosomes requires nucleotide exchange but not effector binding. *Traffic* 12:1056–1066.



- Templer RH, Castle SJ, Curran AR, Rumbles G, Klug DR. 1998. Sensing isothermal changes in the lateral pressure in model membranes using di-pyrenyl phosphatidylcholine. *Faraday Discuss* 41–78.
- Tortorella D, Ulbrandt ND, London E. 1993. Simple centrifugation method for efficient pelleting of both small and large unilamellar vesicles that allows convenient measurement of protein binding. *Biochemistry* 32:9181–9188.
- Ullrich O, Horiuchi H, Bucci C, Zerial M. 1994. Membrane association of Rab5 mediated by GDP-dissociation inhibitor and accompanied by GDP/GTP exchange. *Nature* 368: 157–160.
- Ullrich O, Stenmark H, Alexandrov K, Huber LA, Kaibuchi K, Sasaki T, et al. 1993. Rab GDP dissociation inhibitor as a general regulator for the membrane association of rab proteins. *J Biol Chem* 268:18143–18150.
- Winterhalter M, Helfrich W. 1988. Effect of surface charge on the curvature elasticity of membranes. *J Phys Chem* 92:6865–6867.
- Wu Y-W, Oesterlin LK, Tan K-T, Waldmann H, Alexandrov K, Goody RS. 2010. Membrane targeting mechanism of Rab GTPases elucidated by semisynthetic protein probes. *Nat Chem Biol* 6:689.
- Wu Y-W, Tan K-T, Waldmann H, Goody RS, Alexandrov K. 2007. Interaction analysis of prenylated Rab GTPase with Rab escort protein and GDP dissociation inhibitor explains the need for both regulators. *PNAS* 104:12294–12299.
- Yokoyama K, Kaji H, He J, Tanaka C, Hazama R, Kamigaki T, et al. 2011. Rab27a negatively regulates phagocytosis by prolongation of the actin-coating stage around phagosomes. *J Biol Chem* 286:5375–5382.
- Zerial M, McBride H. 2001. Rab proteins as membrane organizers. *Nat Rev Mol Cell Biol* 2:107–117.

### Supplementary material available online

Supplementary Figures S1–S3.